J Mater Sci (2019) 54:1153–1161

Ceramics

Large and temperature-insensitive piezoelectric strain in xBiFeO$_3$–(1−x)Ba(Zr$_{0.05}$Ti$_{0.95}$)O$_3$ lead-free piezoelectric ceramics

Dongyan Fu[1], Zhenhai Ning[1], Dongli Hu[1], Jinrong Cheng[1], Feifei Wang[2], and Jianguo Chen[1,*]

[1] *School of Materials Science and Engineering, Shanghai University, Shanghai 200444, China*
[2] *Key Laboratory of Optoelectronic Material and Device, Department of Physics, Shanghai Normal University, Shanghai, China*

Received: 6 July 2018
Accepted: 12 September 2018
Published online: 17 September 2018

ABSTRACT

Lead-free piezoelectric materials of xBiFeO$_3$–(1−x)Ba(Zr$_{0.05}$Ti$_{0.95}$)O$_3$–1.0 mol%MnO$_2$ (BF–BZT) ($0.62 \le x \le 0.74$) were prepared by the traditional solid-state reaction process. The structure and high-temperature dielectric, ferroelectric as well as piezoelectric properties were investigated. X-ray diffraction analysis showed that BF–BZT ceramics exhibited pure perovskite structure with the coexistence of tetragonal and rhombohedral phases. Measurements of temperature-dependent dielectric permittivity revealed that BF–BZT ceramics gradually changed from the classical ferroelectrics to relaxors with increasing BZT content. The Curie temperature T_C, coercive electric field E_c (80 kV/cm) and remnant polarization P_r (80 kV/cm) of 0.64BF–0.36BZT ceramics were 370 °C, 27.8 kV/cm and 24.22 μC/cm^2, respectively. The unipolar strain of 0.64BF–0.36BZT reached up to 0.29% (d^*_{33} = 485 pm/V), and the variation of temperature-dependent piezoelectric strain for 0.64BF–0.36BZT was about 17% from 50 to 180 °C, which was only 1/3, 1/2 and 1/10 of the BF–BT-, PZT-5H- and BNT-based piezoelectric ceramics, showing excellent thermal stability. These results indicated that BF–BZT ceramics were competitive candidates for lead-free piezoelectric applications.

Introduction

Pb-based ceramics with excellent piezoelectric and dielectric properties dominated the piezoelectric device market. However, grave environmental pollution caused by using toxic Pb element prompted the exploitation of high-performance lead-free alternatives [1–10]. Recently, lead-free (K, Na)NbO$_3$-based (KNN), (Bi$_{0.5}$Na$_{0.5}$)TiO$_3$–BaTiO$_3$ (BNT–BT), Ba(Ti, Zr)O$_3$-(Ba, Ca)TiO$_3$-based (BZT–BCT) and BiFeO$_3$–BaTiO$_3$ (BF–BT) solid solutions were investigated extensively [11–14]. BNT-based solid solutions exhibit huge electric-field-induced strain (~ 0.35%), good repeatability and high Curie temperature (T_C ~ 300 °C). Unfortunately, the depolarization temperature (T_d ~ 100 °C) is low [15], and strain

Address correspondence to E-mail: kpfocus@shu.edu.cn

https://doi.org/10.1007/s10853-018-2926-8

hysteresis is as large as 60%. The existence of cubic–tetragonal–rhombohedral (C–T–R) three-phase point makes BZT–BCT system excellent ferroelectric properties comparable with lead-based materials [16]. However, the low Curie temperature of about 100 °C limits the real application. Apart from BZT–BCT, the piezoelectric and dielectric characteristics for potassium sodium niobate (KNN)-based piezo-ceramics are very sensitive to the temperature because of the polymorphic phase transition point $T_{O–T}$ below T_C. $BiFeO_3$–$BaTiO_3$ (BF–BT) solid solutions are rhombohedral phase at high BF content, changed to pseudo-cubic structure at 67 mol% BF, and then become tetragonal phase for BF content less than 8 mol% [17]. The Curie temperature of BF–BT materials near the MPB is about 500 °C, much higher than those of KNN-, BNT-BT- and BCT–BZT-based solid solutions. Furthermore, there is no phase transition below the Curie temperature, indicating good temperature-dependent dielectric and piezoelectric properties.

The dielectric, ferroelectric and piezoelectric properties of pure BF–BT ceramics were rarely reported because of the low resistivity caused by oxygen vacancies and mixed Fe^{3+}/Fe^{2+} valence state. The Mn modification was able to increase the DC resistivity of BF–BT ceramics significantly from 2.7×10^7 up to 7.6×10^{12} Ω cm [11]. Then, many other cations, such as Zr, Cu, Cr, Ga, Al and Zn, were further introduced into the BF–BT system to tailor the electrical properties [11, 18–23]. Our previous work showed that the strain of Zr-doped 0.75BF–0.25BT ceramics with rhombohedral phase was enhanced obviously as large as 0.27% [18]. However, the driving field of 0.75BF–0.25BT ceramics reaches as high as 100 kV/cm, 4–5 times those of the commercial PZT ceramics. As well known, the driving electric field of the components near the MPB is usually smaller than those compositions with single rhombohedral or tetragonal phase because the domain wall is easy to switch at the MPB with the coexistence of the two phases. Besides, large strain is normally obtained in the piezoelectric relaxors, which is attributed to the reversible transition of the nano-domains [24–28]. Dielectric relaxation behavior of BF–BT system was reported for phase transition compositions of $x < 0.7$ [29]. In addition, high-temperature dielectric, ferroelectric and piezoelectric properties of piezoelectric materials are highly concerned for a real application. Therefore, in this work, we tailored the BF content in the Zr-modified BF–BT ceramics to decrease the driving electric field and studied the high-temperature dielectric, ferroelectric and piezoelectric properties. As expected, the enlarged piezoelectric strain and reduced coercive field were obtained in the MPB compositions. The temperature-dependent strain of BF–BZT near the phase transition is stable from room temperature to 180 °C.

Experimental procedure

The $xBiFeO_3$–$(1-x)Ba(Zr_{0.05}Ti_{0.95})O_3$–1 mol%$MnO_2$ ($0.62 \le x \le 0.74$) piezoelectric ceramics were prepared by the traditional solid-state reaction process. The raw materials were ZrO_2 (99%), Fe_2O_3 (99%), $BaCO_3$ (99%), MnO_2 (99%), Bi_2O_3 (99%) and TiO_2 (99%). 1 mol% Bi_2O_3 was added in the mixing process to compensate the volatilization of Bi_2O_3 during heat treatment. After weighing following the stoichiometric proportion, the mixture is ball-milled for 24 h and then calcined at 750 °C for 240 min. Under the pressure of 150 MPa, the powder was pressed into pellets with a diameter of 12 mm and thickness of 1 mm. The green pellets were burned at 600 °C to remove the binder and then sintered at 1000–1020 °C for 120 min. Archimedes method was used to estimate the bulk density. X-ray diffraction (Rigaku-D/MAX-2000) was used to analyze the phase structure. To measure the electric properties, sintered ceramic pellets were polished down to 0.4 mm and silver electrodes were fired on the two main faces. The capacitance and dielectric loss were measured by Agilent impedance analyzer (Agilent 4294A). Computer-controlled temperature dielectric spectrum test system was used to measure the high-temperature dielectric properties from 10^2 to 10^6 Hz frequencies. Electric-field-induced strains and ferroelectric hysteresis loops were measured by the ferroelectric testing system (TF1000 analyzer). The high field strain coefficient d^*_{33} was worked out from the applied electric field and the unipolar strain value. Polarization was carried out in a direct current field of 70 kV/cm and in a 120 °C silicone oil for 15 min. After poled, the specimens were aged for 24 h. The piezoelectric constant d_{33} of the sample was measured by a quasi-static piezoelectric meter.

Results and discussion

The X-ray diffraction patterns (XRD) of BF–BZT ceramics at $0.62 \leq x \leq 0.74$ are presented in Fig. 1. All the specimens show pure perovskite structure without the appearance of the second phase. The magnified patterns (Fig. 1b) show the range from 44° to 46°. The peaks of $(002)_T$, $(200)_R$ and $(200)_T$ merge into one peak with increasing BF content, which means a phase transformation from the coexistence of tetragonal and rhombohedral phases with $0.62 \leq x < 0.72$ to single rhombohedral phase with $0.72 \leq x \leq 0.74$ for BF–BZT ceramics. The coexistence of rhombohedral and tetragonal phases is at the BT content of $x = 0.72$. Similar results were observed in Bi(Fe, Ga)O_3–$BaTiO_3$, Bi(Mg, Ti)O_3–$BiFeO_3$–$BaTiO_3$ and $BiFeO_3$–$x$$Ba_{0.70}Sr_{0.30}TiO_3$ solid solutions [30, 31]. Previous work showed that the phase transition point of BF–BT ceramics was at the BF content of 0.7. These results suggest that Zr doping moves the MPB- to BF-rich direction.

Figure 2a–d exhibits the scanning electron micrograph (SEM) images of BF–BZT (x = 0.64–0.70) ceramics derived from fresh fracture surface. The relative densities of all specimens are above 95%, and almost no pores are observed. The grain size decreased slightly from 5–6 μm ($x = 0.64$) to 2–3 μm ($x = 0.70$).

The temperature dependence of dielectric constant ε_r and loss tan δ of BF–BZT ceramics are shown in Fig. 3a. The Curie temperature T_c of BF–BZT ceramics enhances from 355 to 485 °C with BF content increasing from 0.62 to 0.72. The tan δ of BF–BZT is much smaller than that of BF–BT reported by Zhang et al. [29]. Figure 3b shows the frequency- and temperature-dependent dielectric spectrum of BF–BZT ceramics with selected compositions. The dielectric peaks become round and sensitive to the measuring frequency with increasing BF content, showing diffused phase transition features. The degree of dispersion is commonly estimated according to the two parameters: ΔT_{relax}, which means the difference between the two T_m values measured at 1 kHz and 1 MHz, and the diffuseness degree γ derived by the modified Curie–Weiss law, as demonstrated in Fig. 3c.

$$\Delta T_{relax} = T_{m,1MHz} - T_{m,1kHz} \quad (1)$$

$$1/\varepsilon - 1/\varepsilon_m = (T - T_m)^\gamma / C. \quad (2)$$

The C and γ are constant and γ ranges from 1 (typical ferroelectric) to 2 (typical relaxor). The calculated γ for the compositions of $x < 0.66$ is near to 2, implying that BF–BZT ceramics are relaxors.

Figure 4a–e shows ferroelectric and piezoelectric strain of the BF–BZT ceramics at room temperature. The BF–BZT ceramics present typical ferroelectric hysteresis loops without leakage problems. The applied electric field of BF–BZT ceramics is 80 kV/cm (1 Hz), higher than other chemically modified BF–BT ceramics and two or three times of commercial PZT materials. Figure 4b shows the variation of coercive field E_c and residual polarization P_r along with various BF contents. The maximum of E_c is approximately 40 kV, much larger than those of BS-PT, PZT, BLGF-PT and KNN ceramics, suggesting that BF–BZT ceramics have steady domain configuration. The coercive field E_c decreases with the reduction in BF content, which is in accordance with the previously reported rules of BF–BT system [29].

The bipolar and unipolar strain hysteresis loops of BF–BZT are shown in Fig. 4c, d. The standard butterfly curve is observed. The bipolar strain of BF–BZT ceramics reaches up to 0.291% ($x = 0.64$), much higher than those reported in the previous studies (∼ 0.153%) [32], and it is comparable to BS-PT (∼ 0.28%) [33]. It is noted that the BF–BZT is lead free and cheaper than BS-PT. The coercive field of 0.64BF–0.36BZT ceramics is 1/2 of 0.75BF–0.25BZT ceramics because the composition is near phase transition. Furthermore, BF–BZT ceramics with BF content of 0.64 show relaxor behavior in temperature-dependent spectra, implying polar nano-regions

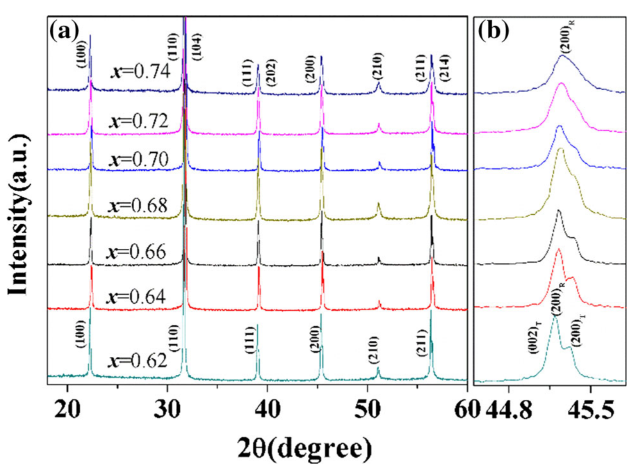

Figure 1 X-ray diffraction of xBF–BZT (x = 0.62–0.74) ceramics.

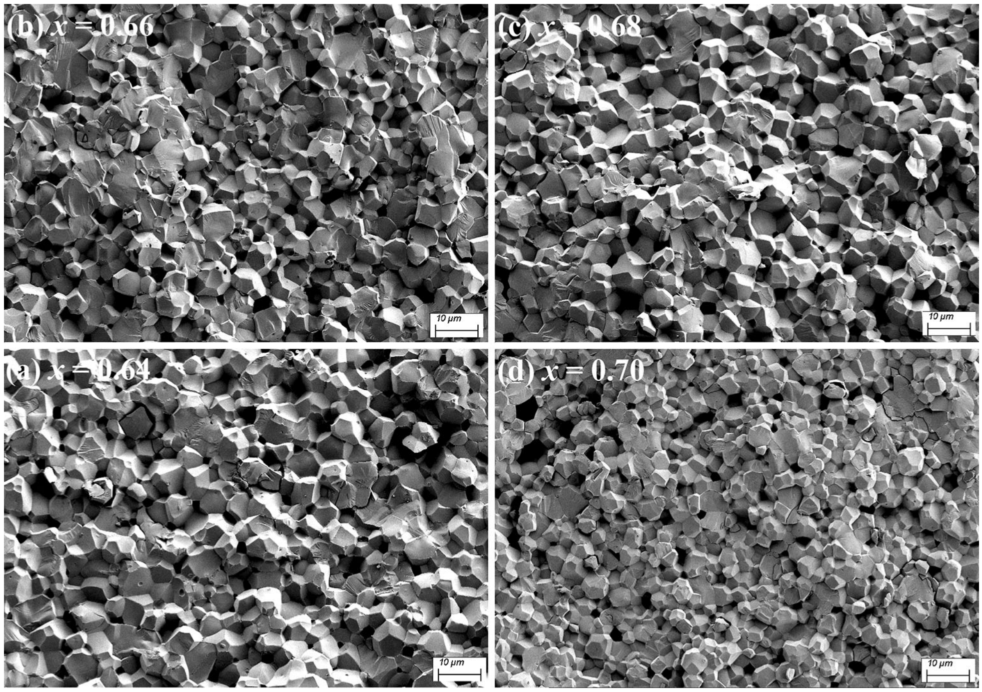

Figure 2 Scanning electron micrograph images of *x*BF–BZT (x = 0.64–0.70) ceramics.

(PNRs) in the solid solutions. Spontaneous polarization in PNRs is easier to rotate, resulting in large strain enhancement [34]. In addition, the strain hysteresis is calculated by the following equation:

$$H_{rel} = H_{Emax/2}/S_{max}, \quad (3)$$

where H_{rel} is strain hysteresis and $H_{Emax/2}$ is different strain values with rising and falling fields at half maximum electric field. The strain hysteresis of 0.64BF–0.36BZT specimen is around 37.8% at 60 kV/cm, which is much smaller than some BNT-based relaxor ferroelectrics (normally larger than 60%). Therefore, the 0.64BF–0.36BZT ceramics can be a candidate for lead-free and low-priced piezoelectric actuator applications.

The variations of positive strain S_{pos}, negative strain S_{neg}, total strain S, peak-to-peak strain and S_{rem}/S for BF–BZT ceramics with increased BF content are offered in Fig. 4e. The S_{neg} is decided by the difference between the maximum negative strain and strain under zero electric field at bipolar strain loops, mostly regarded as remnant strain (S_{rem}), which was measured in the first measurement cycle. The S_{neg} is derived from the reorientation of the ferroelectric domain the contribution of the switching of nonreciprocal non-180° domains. According to the calculation: S_{rem}/S, the contribution of irreversible domain inversion and domain wall movement to total strain can be calculated, which is obtained to be 71% for 0.70BF–0.30BZT ceramics, comparable to the contribution reported in Pb(Zr, Ti)O_3 and $BaTiO_3$ polycrystalline ferroelectric (about 45–80%) [35].

The temperature dependence of unipolar strain curve of *x*BF–BZT ferroelectric under 50 kV/cm for x = 0.64, 0.70 is demonstrated in Fig. 5a, b. The piezoelectric strain and large signal d^*_{33} with temperature are shown in Fig. 5c. The high field strain coefficient d^*_{33}, depicting the strain values under a unit of electric field, is obtained by the following equation:

$$d^*_{33} = S_{max}/E_{max}, \quad (4)$$

where S_{max} is the largest strain and E_{max} is the highest applied electric field. It is obvious that the unipolar strains for each composition are monotonously enhanced with temperature increase from room temperature to 180 °C. Zr-doped BF–BT ceramics can withstand the electric field of 50 kV/cm even at 180 °C and higher than the previously reported 40 kV/cm of *x*BF–BT–Mn ceramics [32]. The Zr^{4+} cations possess higher chemical stability than that of the Ti^{4+} cations, and the Zr^{4+} cations in BF–BT solid solutions may restrain the reaction of $Ti^{4+}+-e^{-}\rightarrow Ti^{3+}$, diminish the defect dipole and space

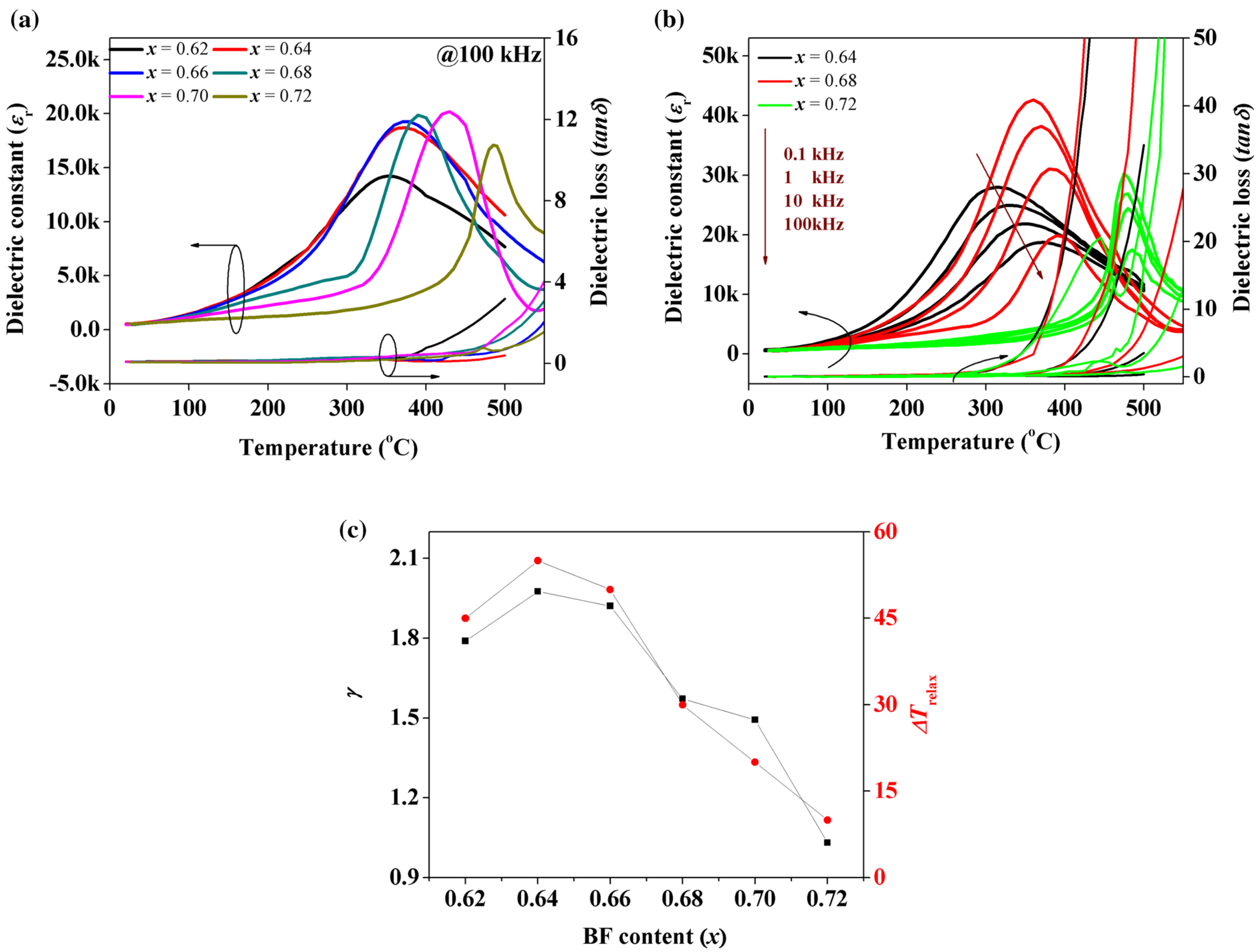

Figure 3 **a** Dielectric loss tanδ and dielectric constant ε_r versus temperature in xBF–BZT ceramics at 100 kHz, **b** dielectric temperature spectrum at different frequencies for xBF–BZT ceramics, **c** the variation of ΔT_{relax} and γ with various BF contents.

charges effectively and improve insulation [36]. Meanwhile, the large field strain close to 0.312% and d^*_{33} value of 624 pm/V are acquired while x = 0.64, which are nearly two times of the 0.67BF–BT–Mn ceramics (0.159%, 396 pm/V) at 180 °C [32]. The enhanced field-induced strain with rising temperature may due to the easier motion of PNRs and domain walls with increasing temperature. Besides, the temperature-dependent strain is a vital parameter for actuator application.

The values of unipolar strain and d^*_{33} versus temperature are summarized in Fig. 5c. The variation rate of d^*_{33} is obtained by the following ratio: $\Delta d^*_{33}/d^*_{33(RT)}$. The variation rate of d^*_{33} versus temperature for diverse piezoelectric materials is listed in Table 1. The variation rate of d^*_{33} for 0.64BF–0.36BT ceramics is within 24% with the temperature ranging from RT to 180 °C. It is noted that the variation rate of piezoelectric strain with temperature for 0.64BF–0.36BZT ceramics is superior to those of PZT-5H ceramics of 40%, 0.67BF–0.33BT–Mn ceramics of 70% and BNT-based relaxor ferroelectrics of 273% [37, 38]. When the temperature ranges from 50 to 180 °C, the variation rate of d^*_{33} for 0.64BF–0.36BT ceramics is within 17%. Those results suggest that the 0.64BF–0.36BZT ceramics possess better thermal stability.

Summary

The xBiFeO$_3$–(1−x)Ba(Zr$_{0.05}$Ti$_{0.95}$)O$_3$ (BF–BZT) piezoelectric ceramics were prepared, and the temperature-dependent electrical properties of BF–BZT materials were studied. With the increase in BF content, phase structures of BF–BZT ceramics transfer from the coexistence of tetragonal and rhombohedral

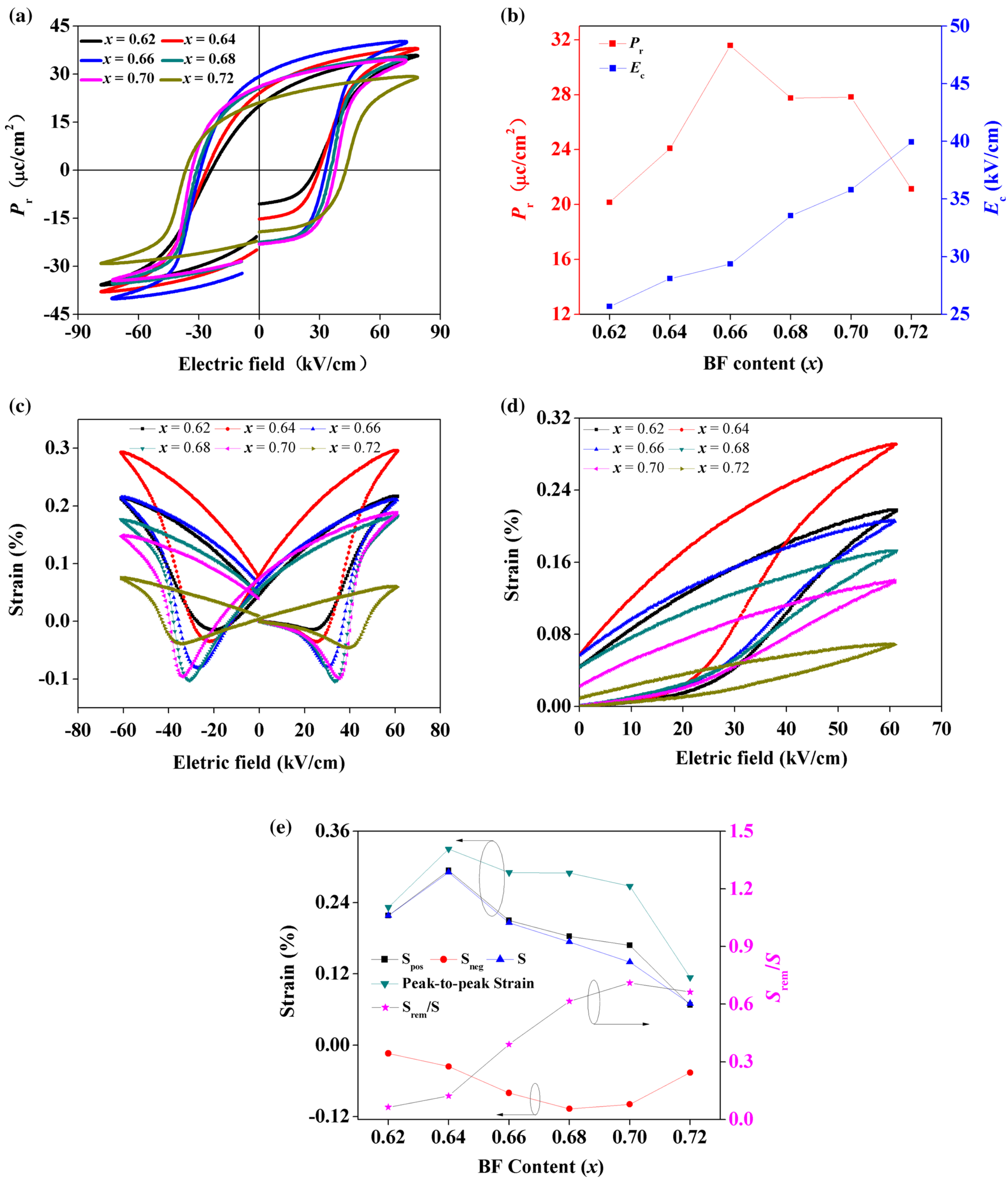

Figure 4 **a** Ferroelectric hysteresis loops, **b** variation of P_r and E_c, **c** bipolar strain loops, **d** unipolar strain loops. **e** The variation of S_{pos}, S_{neg}, S, peak-to-peak strain and S_{rem}/S with different BF contents.

phase with $0.62 \le x < 0.72$ to single rhombohedral with $0.72 \le x \le 0.74$. The large and temperature-dependent strains were obtained for BF–BZT ceramics with the composition of $x = 0.64$. The bipolar

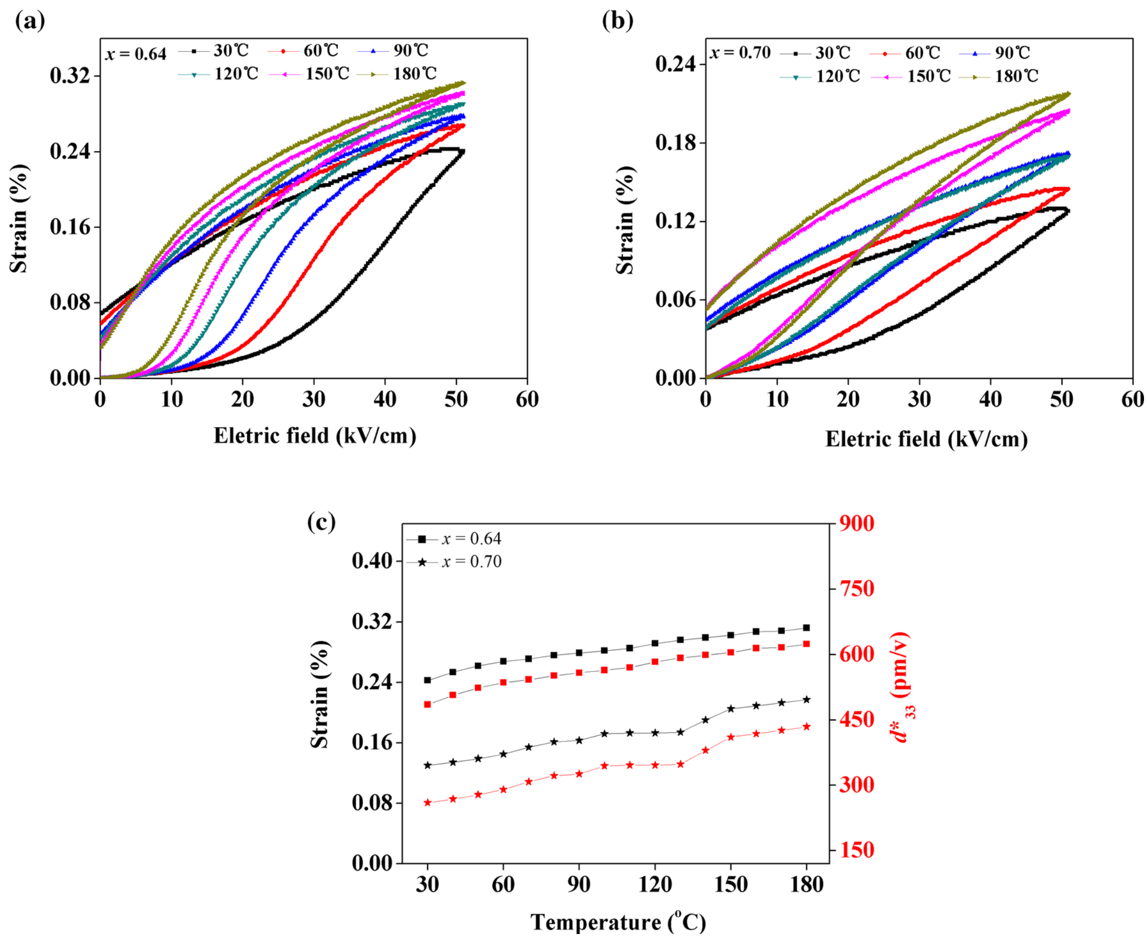

Figure 5 Unipolar strain variation versus temperature in xBF–BZT ceramics at 10 Hz with **a** $x = 0.64$, **b** $x = 0.70$, **c** the strain and d^*_{33} versus temperature under 50 kV/cm.

Table 1 Variation rate of d^*_{33} versus temperature for diverse piezoelectric materials

Materials	Temperature range (°C)	Variation rate of d^*_{33} (%)	Reference
BF	RT-262 °C	258	[39]
0.67BF–0.33BT	RT-180 °C	70	[32]
0.70BF–0.30BT	RT-180 °C	141	[32]
0.64BF–0.36BZT	RT-180 °C	24	This work
0.70BF–0.30BZT	RT-180 °C	59	This work
BNT–BT–BKT	RT-100 °C	273	[38]
PZT-4	RT-160 °C	15	[7]
PZT-5H	RT-80 °C	> 40	[40]

strain, unipolar strain and d^*_{33} of $x = 0.64$ at room temperature were 0.33%, 0.29% and 485 pm/V, respectively. The variation of strain with temperature for BF–BZT ceramics is much smaller than those of BF–BT-, PZT- and BNT–BT-based piezoelectric ceramics. The large and temperature-independent piezoelectric strain indicated that BF–BZT ceramics are competitive candidates for high-temperature lead-free piezoelectric devices.

Acknowledgement

This work was supported by the National Natural Science Foundation of China (Grant No. 51302163, 51672169) and the Innovational Foundation of Shanghai University (Grant No. K. 10-0110-13-009).

Compliance with ethical standards

Conflict of interest The authors declare that they have no conflict of interest.

References

[1] Park SE, Shrout TR (1997) Ultrahigh strain and piezoelectric behavior in relaxor based ferroelectric single crystals. J Appl Phys 82:1804–1811

[2] Hollenstein E, Davis M, Damjanovic D et al (2005) Piezoelectric properties of Li- and Ta-modified $(K_{0.5}Na_{0.5})NbO_3$ ceramics. Appl Phys Lett 87:1829051–1829053

[3] Ang C, Yu Z, Jing Z, Guo R, Cross LE et al (2002) Piezoelectric and electrostrictive strain behavior of Ce-doped $BaTiO_3$ ceramics. Appl Phys Lett 80:3424–3426

[4] Zhang S, Xia R, Shrout TR, Zang G et al (2006) Piezoelectric properties in perovskite $0.948(K_{0.5}Na_{0.5})NbO_3$–$0.052LiSbO_3$ lead-free ceramics. J Appl Phys 100:1041081–1041086

[5] Sabolsky EM, James AR, Kwon S, Messing GL et al (2001) Piezoelectric properties of <001> textured $Pb(Mg_{1/3}Nb_{2/3})O_3$-$PbTiO_3$ ceramics. Appl Phys Lett 78:2551–2553

[6] Sabolsky EM, Trolier-McKinstry S et al (2003) Dielectric and piezoelectric properties of <001> fiber-textured $0.675Pb(Mg_{1/3}Nb_{2/3})O_3$–$0.325PbTiO_3$ ceramics. J Appl Phys 93:4072–4080

[7] Yasuyoshi S, Hisaaki T, Tani T, Kazumasa T, Homma T (2004) Lead-free piezoceramics. Nature 432:84–87

[8] Kroutvar M, DucommunY HD, Bichler M, Schuh D, Abstreiter G, Finley JJ (2004) Optically programmable electron spin memory using semiconductor quantum dots. Nature 432:81–84

[9] Ren X (2004) Large electric-field-induced strain in ferroelectric crystals by point-defect-mediated reversible domain switching. Nat Mater 3:91–94

[10] Wang K, Yao FZ, Jo W et al (2013) Temperature-insensitive (K, Na)NbO3-based lead-free piezoactuator ceramics. Adv Funct Mater 23:4079–4086

[11] Leontsev SO, Eitel RE (2009) Dielectric and piezoelectric properties in Mn-modified $(1-x)BiFeO_3$–$xBaTiO_3$ ceramics. J Am Ceram Soc 92:2957–2961

[12] Zhen YH, Li JF (2006) Normal sintering of (K, Na)NbO3-based ceramics: influence of sintering temperature on densification, microstructure, and electrical properties. J Am Ceram Soc 89:3669–3675

[13] Zhang ST, Bin Y, Cao WW (2012) The temperature-dependent electrical properties of $Bi_{0.5}Na_{0.5}TiO_3$–$BaTiO_3$–$Bi_{0.5}K_{0.5}TiO_3$ near the morphotropic phase boundary. Acta Mater 60:469–475

[14] Acosta M, Novak N et al (2014) Relationship between electromechanical properties and phase diagram in the $Ba(Zr_{0.2}Ti_{0.8})O_3$–$x(Ba_{0.7}Ca_{0.3})TiO_3$ lead-free piezoceramic. Acta Mater 80:48–55

[15] Zhang J, Pan Z, Guo FF, Liu WC, Chen YF (2015) Semiconductor/relaxor 0-3 type composites without thermal depolarization in $Bi_{0.5}Na_{0.5}TiO_3$-based lead-free piezoceramics. Nat Commun 6:66151–661510

[16] Liu W, Ren X (2009) Large piezoelectric effect in Pb-free ceramics. Phys Rev Lett 103:2576021–2576024

[17] Kumar MM, Srinivas A, Suryanarayana SV (2000) Structure property relations in $BiFeO_3/BaTiO_3$ solid solutions. J Appl Phys 87:855–862

[18] Chen JG, Cheng JR (2016) High electric-induced strain and temperature-dependent piezoelectric properties of 0.75BF–0.25BZT lead-free ceramics. J Am Ceram Soc 99:536–542

[19] Yang HB, Zhou CR, Liu X (2013) Piezoelectric properties and temperature stabilities of Mn- and Cu-modified $BiFeO_3$–$BaTiO_3$ high temperature ceramics. J Eur Ceram Soc 33:1177–1183

[20] Liu XH, Xu Z, Wei XY, Yao X (2008) Ferroelectric and ferromagnetic properties of $0.7BiFe_{1-x}Cr_xO_3$–$0.3BaTiO_3$ solid solutions. J Am Ceram Soc 91:3731–3734

[21] Zhou Q, Zhou C, Yang H, Yuan C, Fan Q (2013) Piezoelectric and ferroelectric properties of Ga modified $BiFeO_3$-$BaTiO_3$ lead-free ceramics with high curie temperature. J Mater Sci Mater Electron 25:196–201

[22] Cen Z, Zhou C, Yang H, Lupascu DC (2013) Remarkably high-temperature stability of $Bi(Fe_{1-x}Al_x)O_3$–$BaTiO_3$ solid solution with near-zero temperature coefficient of piezoelectric properties. J Am Ceram Soc 96:2252–2256

[23] Tong K, Zhou CR, Wang J, Li QN (2017) Enhanced piezoelectricity and high-temperature sensitivity of Zn-modified BF–BT ceramics by in situ and ex situ measuring. Ceram Int 43:3734–3740

[24] Hao J, Shen B, Zhai J, Liu C, Roedel J (2013) Large strain response in $0.99(Bi_{0.5}Na_{0.4}K_{0.1})TiO_3$–$0.01(K_xNa_{1-x})NbO_3$ lead-free ceramics induced by the change of K/Na ratio in $(K_xNa_{1-x})NbO_3$. J Am Ceram Soc 96:3133–3140

[25] Shi J, Fan H, Liu X, Li Q (2014) Giant strain response and structure evolution in $(Bi_{0.5}Na_{0.5})0.945$–$x(Bi_{0.2}Sr_{0.7□0.1})$-$xBa_{0.055}TiO_3$ ceramics. J Eur Ceram Soc 34:3675–3683

[26] Daniels JE, Jo W, Rödel J, Jones JL (2009) Electric-field-induced phase transformation at a lead-free morphotropic phase boundary: case study in a $93\%(Bi_{0.5}Na_{0.5})TiO_3$–

7%$BaTiO_3$ piezoelectric ceramic. Appl Phys Lett 95:0329041–0329043

[27] Zhao W, Zuo R, Fu J (2014) Temperature-insensitive large electrostrains and electric field induced intermediate phases in $(0.7-x)Bi(Mg_{1/2}Ti_{1/2})O_3$–$xPb(Mg_{1/3}Nb_{2/3})O_3$–$0.3PbTiO_3$ ceramics. J Eur Ceram Soc 34:4235–4245

[28] Jo W, Granzow T, Aulbach E, Rödel J, Damjanovic D (2009) Origin of the large strain response in $(K_{0.5}Na_{0.5})NbO_3$-modified $(Bi_{0.5}Na_{0.5})TiO_3$-$BaTiO_3$ lead-free piezoceramics. J Appl Phys 105:0941021–0941025

[29] Zhang H, Jo W, Wang K, Webber KG (2014) Compositional dependence of dielectric and ferroelectric properties in $BiFeO_3$–$BaTiO_3$ solid solutions. Ceram Int 40:4759–4765

[30] Zhu LF, Zhang BP, Shun L, Zhao GL (2017) Large piezoelectric responses of Bi(Fe, Mg, Ti)O3-BaTiO3 lead-free piezoceramics near the morphotropic phase boundary. J Alloy Compd 727:382–389

[31] Sharma S, Singh V, Anshul A, Siqueiros JM, Dwivedi RK (2018) Structural stability, enhanced magnetic, piezoelectric, and transport properties in $(1-x)BiFeO_3$–$xBa_{0.70}Sr_{0.30}TiO_3$ nanoparticles. J Appl Phys 123:2041021–20410211

[32] Wei J, Fu D, Cheng JR, Chen JG (2017) Temperature dependence of the dielectric and piezoelectric properties of $xBiFeO_3$–$(1-x)BaTiO_3$ ceramics near the morphotropic phase boundary. J Mater Sci 52:10726–10737. https://doi.org/10.1007/s10853-017-1280-6

[33] Eitel RE, Randall CA, Shrout TR, Park SE (2002) Preparation and characterization of high temperature perovskite ferroelectrics in the solid-solution $(1-x)BiScO_3$–$xPbTiO_3$. Jpn J Appl Phys 41:2099–2104

[34] Li F, Zhang S, Yang T et al (2016) The origin of ultrahigh piezoelectricity in relaxor-ferroelectric solid solution crystals. Nat Commun 7:138071–138079

[35] Qin Y, Zhang JL, Zhang SJ (2016) Domain configuration and thermal stability of $(K_{0.48}Na_{0.52})_2(Nb_{0.96}Sb_{0.04})O_3$–$Bi_{0.50}(Na_{0.82}K_{0.18})_{0.50}ZrO_3$ piezoceramics with high d_{33} coefficient. ACS Appl Mater Int 8:7257–7265

[36] Dong L, Stone DS, Lakes RS (2012) Enhanced dielectric and piezoelectric properties of $xBaZrO_3$–$(1-x)BaTiO_3$ ceramics. J Appl Phys 111:0841071–08410710

[37] Wang K, Hussain A, Jo W, Rödel J (2012) Temperature-dependent properties of $(Bi_{1/2}Na_{1/2})TiO_3$–$(Bi_{1/2}K_{1/2})TiO_3$–$SrTiO_3$ lead-free piezoceramics. J Am Ceram Soc 95:2241–2247

[38] Zhang ST, Kounga AB, Aulbach E, Jo W, Rödel J (2008) Lead-free piezoceramics with giant strain in the system $Bi_{0.5}Na_{0.5}TiO_3$–$BaTiO_3$–$K_{0.5}Na_{0.5}NbO_3$. II. Temperature dependent properties. J Appl Phys 103:0341081–0341087

[39] Wang DW, Amir K, Shunsuke M, Antonio F, Quanliang Z (2017) Temperature dependent, large electromechanical strain in Nd-doped $BiFeO_3$–$BaTiO_3$ lead-free ceramics. J Eur Ceram Soc 37:1857–1860

[40] Wang D, Fotinich Y, Carmangreg P (1998) Influence of temperature on the electromechanical and fatigue behavior of piezoelectric ceramics. J Appl Phys 83:5342–5350